Structural and nanomechanical characterization of niobium films deposited by DC magnetron sputtering

X. Li[1] · W. H. Cao[2] · X. F. Tao[1] · L. L. Ren[1] · L. Q. Zhou[3] · G. F. Xu[3]

Abstract Nb thin films were deposited onto Si wafers by direct current (DC) magnetron sputtering at different deposition pressures. The microstructure and nanomechanical properties of Nb films were investigated by scanning electron microscope, X-ray diffractometer, transmission electron microscope, atomic force microscope and nanoindenter. The results revealed that the grain size, thickness, surface roughness, the reduced elastic modulus (Er) and hardness (H) values of Nb thin films increased at the pressure range of 0.61–0.68 Pa. Meanwhile, the porosity of Nb films decreased with the increase in deposition pressure. The lattice deformation of Nb thin films changed from negative to positive with the increase in deposition pressure. It is concluded that deposition pressure influences the microstructure and nanomechanical properties of Nb films.

1 Introduction

Nb thin films have attracted extensive attention of the scientific community for many years for applications in quantum bits (qubit) and photon detectors [1, 2]. The usage of superconducting Nb films for qubit applications is due to their low impedance and low subgap leakage in Josephson junctions. The ultra-thin Nb films can be used to realize the potential high speed of superconducting photon detectors. Many researchers have devoted to optimize film preparation techniques for the purpose of ideal superconductivity [3, 4]. Meanwhile, some experiments have indicated that microstructure (pore, grain size, thickness, etc.) and mechanical properties of Nb thin films exert significant influence on the performance of Nb thin film devices [5, 6]. However, research in this field is not sufficient and some advanced measuring techniques should be employed to study this topic in depth [7, 8]. In this work, we prepared three kinds of Nb thin films on Si wafers by using DC magnetron sputtering deposition at different deposition pressures. The microstructure and nanomechanical properties of the films were investigated using several measurement techniques. The interrelationships among these tested characteristic parameters were revealed by elastic–plastic deformation theories. We devoted to extend this research topic and provide a guide for the designing and producing practice of Nb-based Holzer components.

2 Experimental procedure

Nb thin films were prepared by DC magnetron sputtering deposition (Kurt J. Lesker CMS-A) using a 99.95 % pure Nb target. High purity argon was utilized as sputtering gas, and the temperature of Si wafers was maintained at slightly larger than 20 °C by cooling water flowing inside the pedestal. The Si substrates were separated about 11 cm from the target, and the chamber was pumped to a base pressure of below 1.33×10^{-6} Pa. Nb films were prepared with deposition pressures of 0.61, 0.65 and 0.68 Pa and deposition time of 350 s. The employment of these deposition pressures is based on the result that residual stress in

✉ X. Li
lixu1359@sina.com; li-xu@nim.ac.cn

1 Division of Nano Metrology and Materials Measurement, National Institute of Metrology, Beijing 100029, China

2 Division of Electricity and Magnetism, National Institute of Metrology, Beijing 100029, China

3 School of Materials Science and Engineering, Central South University, Changsha 410083, China

Nb films changed remarkably at the range of 0.61–0.68 Pa in our previous work of measuring stress by curvature method. The microstructure of Nb thin films was studied using a Zeiss Ultra 55 scanning electron Microscope (SEM) equipped with an Oxford X-Max 20 mm^2 energy dispersive X-ray spectrometer. The films were then subjected to grazing incidence X-ray diffraction (XRD) analysis using a PANalytical X-ray diffractometer with incident angle of X-ray = 2° and Cu Kα radiation ($\lambda = 0.15406$ nm). High-resolution electron microscopy (HREM) images of the interface were obtained using a Zeiss Libra 200 field-emission transmission electron microscope (TEM) operated at 200 kV. Geometric Phase Analysis (GPA) Plug-ins (HREM Research Inc.) was used to calculate the deformation of lattice fringes in Nb films. The surface morphology and roughness of Nb thin films were measured by a Dimension Icon atomic force microscopy (AFM). Nanoindentaion tests were lastly performed by a Berkovich indenter with a tip curvature radius of approximate 100 nm in Hysitron TI900 Triboindenter. All tests were done with a depth-control model as one loading–holding–unloading circle indentation with the same holding time of 2 s, while the linearly loading and unloading segment durations were held for 5 s. Based on the ISO and ASTM standards [9], i.e., the maximum indentation depth should not exceed 10 % of the thickness of a film in order to avoid the influence of substrate; the indentation depths of three Nb films were set to 22 nm.

3 Results and discussion

The surface and cross-sectional SEM images of Nb thin films sputtered at different deposition pressures are shown in Fig. 1. For the Nb film deposited at 0.61 Pa, lamellar structure is observed on the Si substrate. These lamellas grow bigger in size with the increase in deposition pressure and lead to the decrease in porosity (Fig. 1c, e). The cross-sectional microstructure of Nb/Si samples consists of three layers and two sharp interfaces. The element line-scan analysis reveals that Nb is mainly distributed in the outermost layer, O in the middle layer and Si in the bulk substrate. The Nb film prepared at pressure of 0.61 Pa, which is characterized of columnar grains and tightly bond to the substrate, has a thickness of approximate 228.9 nm. The thickness of Nb films prepared at 0.65 and 0.68 Pa increases to 401.9 and 471.7 nm, respectively. Meanwhile, the columnar grains grow larger in length with the increase in deposition pressure.

The XRD patterns of Nb thin films deposited at different deposition pressures are shown in Fig. 2, from which we can see the main diffraction crystallographic planes are (110), (200), (211) and (220). The intensity of (110) peak increases remarkably with the increment of deposition pressure, which indicates that the crystallinity is gradually improved in the Nb thin films [10]. It is noted that the phase composition of Nb films changes from single body-centered cubic (bcc Nb) at deposition pressure of 0.65 Pa to mixed phases (bcc Nb and Nb_2O_5) at 0.68 Pa. The formation of Nb_2O_5 is due to the oxidation of Nb, which is proved by earlier researches [11, 12]. The theoretical and experimental interplanar spacings (d) of Nb films are listed in Table 1. It can be seen that the experimental d-spacings of $Nb_{(110)}$ are different with the theoretical value and the biggest deviation is 4.21 %. These deviations are caused by lattice distortion which ultimately produces residual stress in the films.

The HREM images of Nb thin films prepared at different deposition pressures are displayed in Fig. 3. The (110) interplanar spacings of Nb thin films prepared at pressures of 0.61, 0.65 and 0.68 Pa are measured, respectively, to be 0.226, 0.235 and 0.245 nm. They are significantly different with the theoretical value (0.23379 nm), which indicate that residual stress exists in the Nb thin films. By analyzing the HREM image with GPA plug-ins, we measured the deformation of the lattice fringe relative to an internal reference lattice (the white square) in the Nb films, as shown in Fig. 3b, d, f. As expected, the lattice deformations are slightly negative in the Nb films deposited at 0.61 and 0.65 Pa, i.e., the colors of the deformation map in the fringe region are mainly green and blue. However, the lattice deformation is mainly positive in the Nb films deposited at 0.68 Pa.

The surface morphology and roughness of Nb films were obtained by using AFM, which also provided guidance for the parameter design of nanoindentation test. The Nb thin film prepared at 0.61 Pa has a root-mean-square roughness (Rq) of 1.70 nm and a mean surface roughness (Ra) of 1.32 nm. When the deposition pressure of the Nb film is 0.65 Pa, The Rq and Ra of the Nb film are, respectively, 2.28 and 1.81 nm. By increasing the deposition pressure to 0.68 Pa, the Rq and Ra increase to 2.55 and 2.02 nm, respectively. It is concluded that the roughness of Nb films goes up with the increase in deposition pressure. In addition, the morphology of the Nb film prepared at 0.68 Pa presents better crystallinity and larger grain size when compare to the other two Nb films.

The nanomechanical properties of Nb films are presented in Fig. 4. Prior to testing Nb films [13, 14], the fused quartz reference material was utilized to calibrate the area function of the indenter and the machine compliance of the whole instrument. As shown in Fig. 4a, all the actual indentation depths of Nb films prepared at 0.61, 0.65 and 0.68 Pa are about 22 nm. The load–displacement curves of the Nb film prepared at 0.61 Pa display a dispersion feature. It is noted that the peak indentation loads of the Nb

Fig. 1 Surface and cross-sectional SEM images of Nb thin films prepared at **a** and **b** 0.61 Pa, **c** and **d** 0.65 Pa, **e** and **f** 0.68 Pa
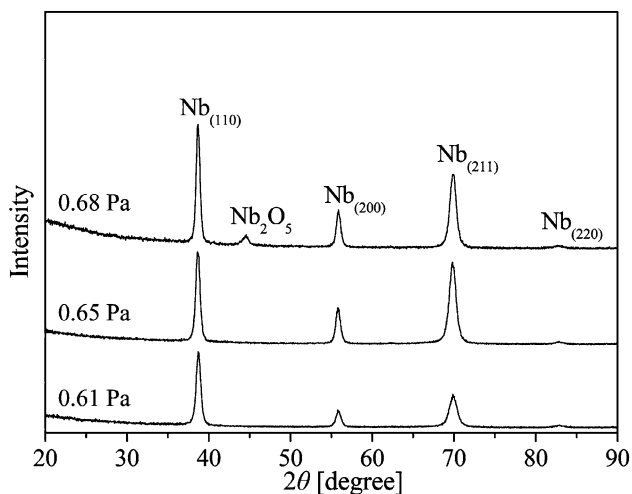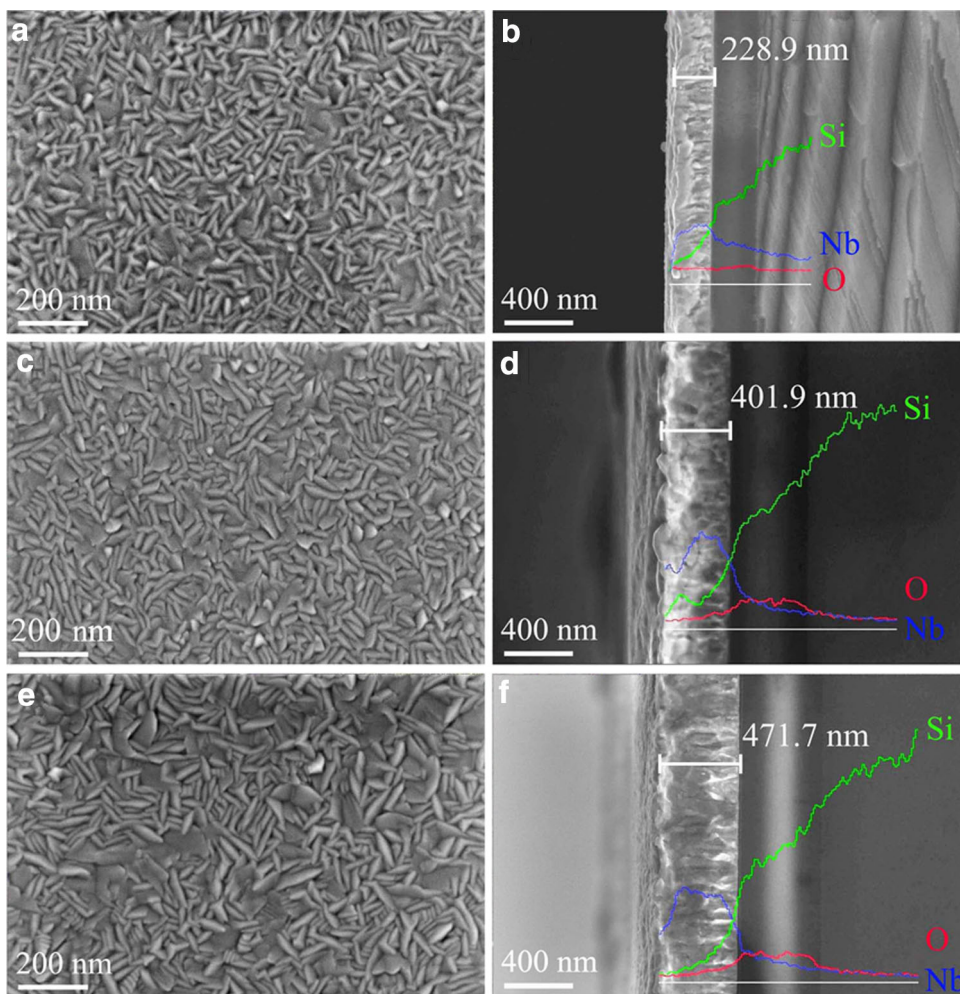

Fig. 2 XRD patterns of Nb thin films prepared at different deposition pressures

have different slopes, which can be used to calculate the Er and H. The Er and H values of Nb films, calculated by using the Oliver and Pharr post treatment method [15], are shown in Fig. 4d. The Er values and corresponding standard deviations of three Nb films are, respectively, 101.43 ± 4.41, 102.32 ± 2.45 and 115.01 ± 2.20 GPa. Meanwhile, the H values are 4.45, 4.82 and 5.39 GPa and have standard deviations of 0.20, 0.26 and 0.15 GPa, respectively. It is concluded that the Er and H values slightly increase with the increase in deposition pressure, while the standard deviations of Er and H generally decrease.

Earlier works have revealed the relationship between the elastic modulus, hardness of a thin film and its porosity [16, 17]:

$$E = E_0 \times e^{(-BP)} \tag{1}$$

$$H = H_0 \times e^{(-bP)} \tag{2}$$

in which E_0 and H_0 are the elastic modulus and hardness of fully dense film, respectively. P was the volume fraction of

films prepared at 0.61 and 0.65 Pa are around 160 μN when the Nb film prepared at 0.68 Pa received a peak load of about 180 μN. The unloading parts of these curves

Table 1 Theoretical and experimental interplanar spacings of Nb thin films

Films (Pa)	$d_{110\ \text{theoretical}}$ (nm)	$d_{110\ \text{experimental}}$ (nm)	Δd_{110} (nm)	δ (%)
0.61	0.23379	0.22576	−0.00803	−3.43
0.65	0.23379	0.23248	−0.00131	−0.56
0.68	0.23379	0.24363	0.00984	4.21

Fig. 3 HREM and fringe deformation of Nb thin films prepared at **a** and **b** 0.61 Pa, **c** and **d** 0.65 Pa, **e** and **f** 0.68 Pa
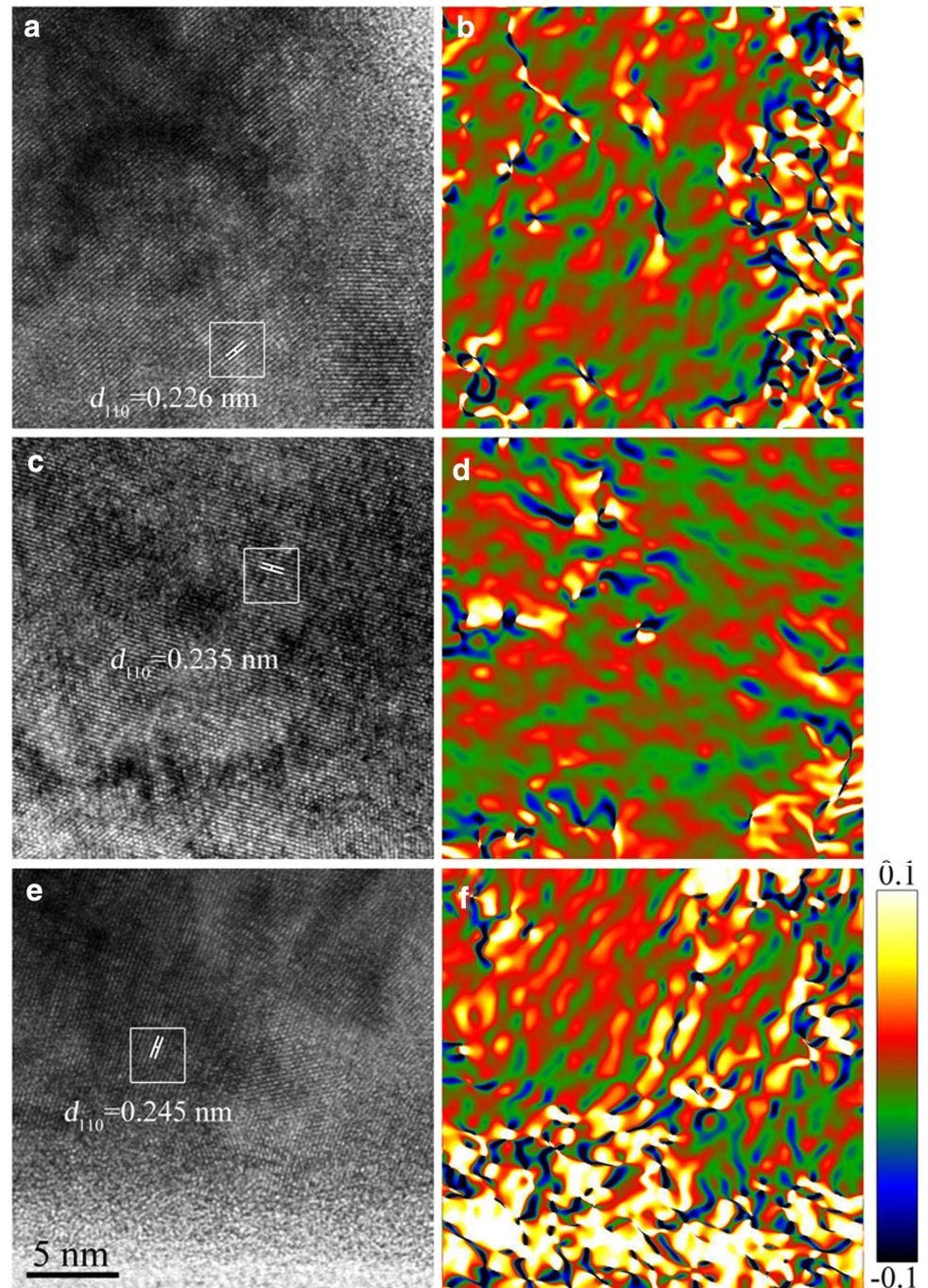
pore. B and b were empirical constants ranging between 2 and 4. The two equations suggested that the decrease in porosity resulted in the increase of E and H. In this work, the porosity of Nb thin films decreases, and the Er and H values increase with the increase in deposition pressure, which can be explained by the equations.
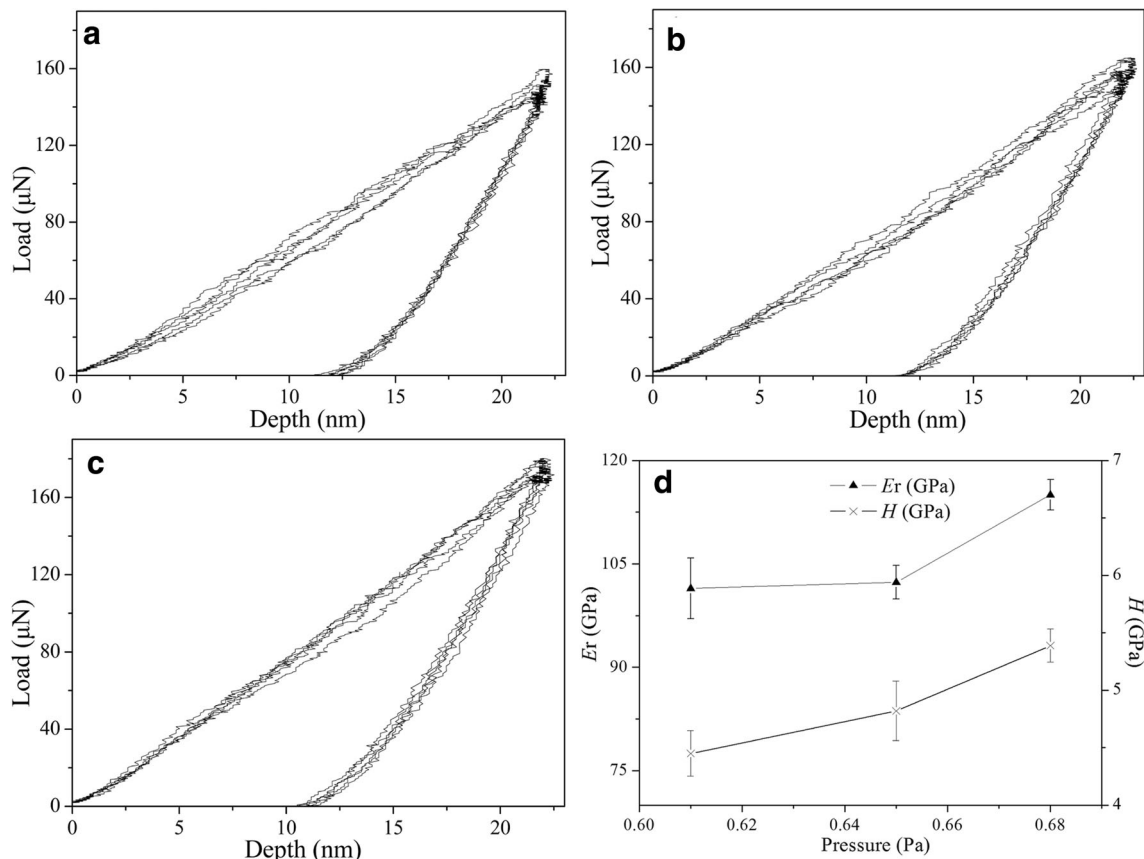
Fig. 4 Load–displacement curves of Nb thin films prepared at **a** 0.61 Pa, **b** 0.65 Pa and **c** 0.68 Pa; **d** Effect of deposition pressure on the reduced elastic modulus and hardness

The effect of grain size on elastic modulus and hardness was significant when the grain size of materials was smaller than 20 nm [18, 19]. In this work, the grain size of three Nb films is mostly larger than 20 nm and thus this effect is negligible. However, the grain size of Nb films can influence the yield stress of slip deformation in nanoindentation test according to the Hall–Petch relationship [20]. The larger the grain size, the smaller the yield stress required for slip deformation. The grain size of Nb films increases with the increase in deposition pressure, and thus slip is most easily activated in the Nb film prepared at 0.68 Pa. That is, the Nb film prepared at 0.61 Pa is the hardest and the Nb film prepared at 0.68 Pa is the softest. The accuracy of nanoindentation test is better in "soft" Nb grains than in "hard" Nb grains. That is exactly why the standard deviations of Er and H decease with the increase in deposition pressure.

According to the XRD and HREM results, the lattice deformation in the Nb thin films changes from compressive to tensile and generally increases during the increase in deposition pressure, which caused by the evolution of microstructure, the difference of thermal properties between film and substrate or other mechanisms. When the residual stress in Nb films is larger than a critical in-plane

stress, interface cracks and delamination morphologies are produced subsequently. Researches have revealed the effect of some factors on the critical in-plane stress [21]:

$$\sigma_{\mathrm{cr}} = \pm|\sigma_{\mathrm{in}}| + \sqrt{\frac{2\gamma E}{D(1 - v^2)}} \tag{3}$$

where σ_{in} was the initial value present after film preparation, E the elastic modulus, γ the adhesion energy per unit area, v the Poisson's ratio of the film and D the film thickness. This equation reveals that the decrease in elastic modulus and the increase in film thickness result in the decrease in the critical stress. That is exactly why film detachment phenomenon more frequently happens with the increase in film thickness. In this work, although detachment phenomenon does not happen in the Nb film obtained at 0.68 Pa, the clear interface indicates that the Nb film tends to detach with a high possibility.

It is of importance to take surface roughness into account in the nanoindentation tests of thin films. Earlier studies suggested that the roughness had a significant influence on the experimental precision of the tests when the characteristic size of roughness was on the order of the indenter, and the indentation load was in the range of

0.2–2 mN [22]. The tested elastic module would be incorrect when the indentation depth was in the range of surface roughness. The rougher the indented surface, the more the energy dissipated during the plastic deformation, and the more significant the indentation size effect. Both the nanohardness and elastic modulus of rough thin films from nanoindentation tests were significantly lower than those predicted for smooth thin films [23]. The finite element method simulation revealed that the hardness and reduced modulus of AISI 316L stainless steel decreased with the rise of surface roughness from 2 to 37 nm. The scatter of load–depth curves and the deviation of hardness and elastic modulus were affected by the changing of roughness [24]. In this work, both the curvature radius and the indentation depth of the indenter are considerably larger than the surface roughness of Nb films; the indentation load is large and the surface roughness changes relatively little. Therefore, the effect of surface morphology on the changing of the nanomechanical properties of Nb films and the experimental precision can be ruled out.

4 Conclusions

The microstructure and nanomechanical properties of Nb thin films deposited at different deposition pressures were studied using several techniques. It was revealed that the grain size, thickness, surface roughness, Er and H values of Nb thin films increased at the pressure range of 0.61–0.68 Pa. Meanwhile, the porosity of Nb films decreased with the increase in deposition pressure. The lattice deformation of Nb thin films changed from negative to positive with the increase in deposition pressure. It is concluded that deposition pressure influences the microstructure and nanomechanical properties of Nb films.

References

1. L.P. Rokhinson, X. Liu, J.K. Furdyna, The fractional a.c. Josephson effect in a semiconductor-superconductor nanowire as a signature of Majorana particles. Nat. Phys. **8**, 795–799 (2012)
2. A.J. Annunziata, D.F. Santavicca, J.D. Chudow, L. Frunzio, M.J. Rooks, A. Frydman, D.E. Prober, Niobium superconducting nanowire single-photon detectors. IEEE Trans. Appl. Supercond. **19**, 327–331 (2009)
3. E. Arslan, Structural, mechanical and corrosion properties of NbN films deposited using dc and pulsed dc reactive magnetron sputtering. Surf. Eng. **26**, 615–619 (2010)
4. A. Casaburi, N. Zen, K. Suzuki, M. Ejrnaes, S. Pagano, R. Cristiano, M. Ohkubo, Subnanosecond time response of large-area superconducting stripline detectors for keV molecular ions. Appl. Phys. Lett. **94**, 212502-1–212502-3 (2009)
5. R. Krishnan, C. David, P.K. Ajikumar, S. Dash, A.K. Tyagi, V. Jayaram, B. Raj, Reactive pulsed laser deposition and characterization of niobium nitride thin films. Surf. Coat. Technol. **206**, 1196–1202 (2011)
6. K. Vasu, M.G. Krishna, K.A. Padmanabhan, Effect of Nb concentration on the structure, mechanical, optical, and electrical properties of nano-crystalline $Ti_{1-x}Nb_x$ N thin films. J. Mater. Sci. **47**, 3522–3528 (2012)
7. M.A.A. Mamun, A.H. Farha, Y. Ufuktepe, H.E. Elsayed-Ali, A.A. Elmustafa, Investigation of the crystal structure on the nanomechanical properties of pulsed laser deposited niobium nitride thin films. J. Mater. Res. **27**, 1725–1731 (2012)
8. C.V. Falub, G. Thorwarth, C. Affolter, U. Müller, C. Voisard, R. Hauert, Quantitative in vitro method to predict the adhesion lifetime of diamond-like carbon thin films on biomedical implants. Acta Biomater. **5**, 3086–3097 (2009)
9. W.C. Oliver, G.M. Pharr, Measurement of hardness and elastic modulus by instrumented indentation: advances in understanding and refinements to methodology. J. Mater. Res. **19**, 3–20 (2004)
10. J.E. Alfonso, J. Buitrago, J. Torres, J.F. Marco, B. Santos, Influence of fabrication parameters on crystallization, microstructure, and surface composition of NbN thin films deposited by RF magnetron sputtering. J. Mater. Sci. **45**, 5528–5533 (2010)
11. P. Periasamy, J.J. Berry, A.A. Dameron, J.D. Bergeson, D.S. Ginley, R.P. O'Hayre, P.A. Parilla, Fabrication and characterization of MIM diodes based on Nb/Nb_2O_5 via a rapid screening technique. Adv. Mater. **23**, 3080–3085 (2011)
12. B. Subramanian, R. Ananthakumar, M. Jayachandran, Effect of substrate temperature on the properties of reactively sputtered TiN/NbN multilayers. Cryst. Res. Technol. **46**, 1273–1282 (2011)
13. P. Lee-Sullivan, Influence of cooling rate on stress relaxation response of strained PVDF film. Mater. Res. Innov. **10**, 124–126 (2006)
14. Y.X. Wang, A. Aljaafari, Y. Ju, W. Gao, Mechanical property of solid ZrO powder enhanced Au–Ni coating. Mater. Res. Innov. **18**, 1132–1136 (2014)
15. W.C. Oliver, G.M. Pharr, An improved technique for determining hardness and elastic modulus using load and displacement sensing indentation experiments. J. Mater. Res. **7**, 1564–1583 (1992)
16. P.G. Sanders, J.A. Eastman, J.R. Weertman, Elastic and tensile behavior of nanocrystalline copper and palladium. Acta Mater. **45**, 4019–4025 (1997)
17. R.W. Rice, Limitations of pore-stress concentrations on the mechanical properties of porous materials. J. Mater. Sci. **32**, 4731–4736 (1997)
18. H.S. Kim, M.B. Bush, The effects of grain size and porosity on the elastic modulus of nanocrystalline materials. Nanostruct. Mater. **11**, 361–367 (1999)
19. S. Bagheri, M. Guagliano, Review of shot peening processes to obtain nanocrystalline surfaces in metal alloys. Surf. Eng. **25**, 3–14 (2009)
20. A. Loucif, R.B. Figueiredo, T. Baudin, F. Brisset, R. Chemam, T.G. Langdon, Ultrafine grains and the Hall–Petch relationship in an Al–Mg–Si alloy processed by high-pressure torsion. Mater. Sci. Eng., A **532**, 139–145 (2012)
21. A. Pundt, E. Nikitin, P. Pekarski, R. Kirchheim, Adhesion energy between metal films and polymers obtained by studying buckling induced by hydrogen. Acta Mater. **52**, 1579–4587 (2004)
22. Y.L. Wang, Z. Lin, J.P. Lin, J.H. Peng, G.L. Chen, Influence of sample surface condition on nano indentation experiment. Rare Met. **21**, 131–132 (2002)
23. W.G. Jiang, J.J. Su, X.Q. Feng, Effect of surface roughness on nanoindentation test of thin films. Eng. Fract. Mech. **75**, 4965–4972 (2008)
24. L. Chen, A. Ahadi, J.M. Zhou, J.E. Ståhl, Modeling effect of surface roughness on nanoindentation tests. Proc. CIRP CMMO **8**, 334–339 (2013)